

**The following resources related to this article are available online at  
[www.sciencemag.org](http://www.sciencemag.org) (this information is current as of November 19, 2009):**

**Updated information and services**, including high-resolution figures, can be found in the online version of this article at:

<http://www.sciencemag.org/cgi/content/full/326/5953/726>

**Supporting Online Material** can be found at:

<http://www.sciencemag.org/cgi/content/full/326/5953/726/DC1>

This article **cites 21 articles**, 8 of which can be accessed for free:

<http://www.sciencemag.org/cgi/content/full/326/5953/726#otherarticles>

This article appears in the following **subject collections**:

Epidemiology

<http://www.sciencemag.org/cgi/collection/epidemiology>

Information about obtaining **reprints** of this article or about obtaining **permission to reproduce this article** in whole or in part can be found at:

<http://www.sciencemag.org/about/permissions.dtl>

8. B. Guo, J. D. Phillips, Y. Yu, E. A. Leibold, *J. Biol. Chem.* **270**, 21645 (1995).
9. F. Samaniego, J. Chin, K. Iwai, T. A. Rouault, R. D. Klausner, *J. Biol. Chem.* **269**, 30904 (1994).
10. K. Iwai *et al.*, *Proc. Natl. Acad. Sci. U.S.A.* **95**, 4924 (1998).
11. K. Yamanaka *et al.*, *Nat. Cell Biol.* **5**, 336 (2003).
12. E. Bourdon *et al.*, *Blood Cells Mol. Dis.* **31**, 247 (2003).
13. E. S. Hanson, M. L. Rawlins, E. A. Leibold, *J. Biol. Chem.* **278**, 40337 (2003).
14. J. Wang *et al.*, *Mol. Cell. Biol.* **24**, 954 (2004).
15. K. B. Zumbrennen, E. S. Hanson, E. A. Leibold, *Biochim. Biophys. Acta* **1783**, 246 (2008).
16. See supporting material on Science Online.
17. N. Zhang *et al.*, *Biochem. Biophys. Res. Commun.* **359**, 34 (2007).
18. A. R. Willems, M. Schwab, M. Tyers, *Biochim. Biophys. Acta* **1695**, 133 (2004).
19. K. Iwai, R. D. Klausner, T. A. Rouault, *EMBO J.* **14**, 5350 (1995).
20. S. L. Clarke *et al.*, *EMBO J.* **25**, 544 (2006).
21. C. Fillebeen, D. Chahine, A. Caltagirone, P. Segal, K. Pantopoulos, *Mol. Cell. Biol.* **23**, 6973 (2003).
22. R. E. Stenkamp, *Chem. Rev.* **94**, 715 (1994).
23. C. E. French, J. M. Bell, F. B. Ward, *FEMS Microbiol. Lett.* **279**, 131 (2008).
24. J. H. Zhang, D. M. Kurtz Jr., Y. M. Xia, P. G. Debrunner, *Biochemistry* **30**, 583 (1991).
25. N. J. Greenfield, *Nat. Protocols* **1**, 2876 (2007).
26. J. M. Galan, M. Peter, *Proc. Natl. Acad. Sci. U.S.A.* **96**, 9124 (1999).
27. D. E. Somers, S. Fujiwara, *Trends Plant Sci.* **14**, 206 (2009).
28. We thank R. Eisenstein for IRP1 reagents and helpful discussions; Z. Chen for SCF expression plasmids; W. Gao for K<sub>0</sub>-GST-Ubiquitin and helpful discussions; M. Brown and J. Goldstein for E2 expression constructs; K. Gardner and F. Correa for assistance with circular dichroism; the UTSW HTS facility for assistance with siRNA screening; and L. Wang, G. Pineda, S. Laxman, X. Du, and J. Wang

for helpful discussions. R.K.B. is the Michael L. Rosenberg Scholar in Medical Research and was supported by the Burroughs Wellcome Fund, the Robert A. Welch Foundation, the Texas Advanced Research Program, and NIH grant CA115962. This investigation was conducted in a facility constructed with support from the Research Facilities Improvement Program (grant C06 RR 15437-01) from the NIH National Center for Research Resources.

#### Supporting Online Material

[www.sciencemag.org/cgi/content/full/1176326/DC1](http://www.sciencemag.org/cgi/content/full/1176326/DC1)  
Materials and Methods

Figs. S1 to S8

Tables S1 to S6

References

14 May 2009; accepted 26 August 2009

Published online 17 September 2009;

10.1126/science.1176326

Include this information when citing this paper.

# Quantifying the Impact of Immune Escape on Transmission Dynamics of Influenza

Andrew W. Park,<sup>1,2\*</sup> Janet M. Daly,<sup>3,4</sup> Nicola S. Lewis,<sup>3,5,6</sup> Derek J. Smith,<sup>5,7,8</sup>  
James L. N. Wood,<sup>6</sup> Bryan T. Grenfell<sup>7,9,10</sup>

Influenza virus evades prevailing natural and vaccine-induced immunity by accumulating antigenic change in the haemagglutinin surface protein. Linking amino acid substitutions in haemagglutinin epitopes to epidemiology has been problematic because of the scarcity of data connecting these scales. We use experiments on equine influenza virus to address this issue, quantifying how key parameters of viral establishment and shedding increase the probability of transmission with genetic distance between previously immunizing virus and challenge virus. Qualitatively similar patterns emerge from analyses based on antigenic distance and from a published human influenza study. Combination of the equine data and epidemiological models allows us to calculate the effective reproductive number of transmission as a function of relevant genetic change in the virus, illuminating the probability of influenza epidemics as a function of immunity.

As well as occasional pandemics caused by novel virus subtypes against which the population has no natural immunity, influenza virus causes annual epidemics in man, resulting in considerable morbidity and mortality (1). The recurring dynamics of annual influenza arises largely from the evolution of the virus (2) [particularly gradual changes in the

surface antigens, haemagglutinin (HA), and neuraminidase, which determine the influenza subtype]. The mutation rate of the H3N2 subtype of human influenza A virus, which has caused most morbidity and mortality between 1968 and 2009, results in the appearance of antigenically novel viruses every 2 to 5 years (3). These viruses have amino acid substitutions at key antigenic sites, allowing them to escape the humoral immunity of individuals vaccinated or infected with preceding strains.

Integration of the epidemiological and evolutionary dynamics (phylogenetics) of influenza viruses is much studied (3–7). However, a crucial gap in our knowledge is that we do not know how changes in viral HA translate into immune escape in previously infected or vaccinated hosts, in terms of increases in the effective reproductive number (8). To quantify this relationship, we need data from controlled seasonal influenza infections, preferably of a natural mammalian host with manipulated prior immunity. A series of experimental infection studies with equine influenza virus (EIV) provides this opportunity (table S1).

Equine influenza vaccines have been used, particularly in racehorses, since the 1960s. For more than 40 years, all equine influenza infections have been caused by strains of the H3N8 subtype, which has a similar course of infection to seasonal influenza A in humans (9). In the late 1980s, and in contrast to influenza A in humans, the equine H3N8 subtype diverged into two lineages (10). Experiments in which homologous and heterologous equine influenza vaccines were tested (11) allow us to relate the impact of differences between vaccine and challenge strains on key epidemiological parameters. We begin with the simplest model, using amino acid substitutions (genetic distance) to measure heterology of different strain pairs (11). Our focus here is on relating broad patterns of heterology to epidemic risk. Outbreaks can occur in a wholly susceptible population when the basic reproductive number ( $R_0$ ) exceeds one; that is, an infectious individual gives rise, on average, to more than one new infection (8). In populations that are not wholly susceptible (for example, a partially vaccinated population), the effective reproductive number,  $R$ , which takes into account that infectious individuals may make contact with nonsusceptible individuals, is the more appropriate measure of outbreak risk (8). The effective reproductive number can be calculated as  $R = R_0 p q d / d_{\max}$ , where  $p$  and  $q$  are the probabilities of becoming infected and infectious, respectively, and  $d$  is the infectious period (11). The parameter  $d_{\max}$  is the maximum infectious period (estimated as the sample mean of the control animals).

The equine data (Fig. 1) show that even when the HAs of the vaccine and challenge strains are identical, the nonadjuvanted vaccines used are imperfect; animals vaccinated with a homologous strain have ~55% chance of becoming infected ( $p$ ) and, if infected, have ~65% chance of becoming infectious ( $q$ ), and are infectious ( $d$ ) for an average of 2.8 days. Figure 1 also shows that  $p$ ,  $q$ , and  $d$  increase with increasing number of amino acid differences in antigenic sites,  $a$  [supported by regression analyses (table S2)]. For mismatches of five or more amino acids in

<sup>1</sup>Odum School of Ecology, University of Georgia, Athens, GA 30602, USA. <sup>2</sup>Department of Infectious Diseases, College of Veterinary Medicine, University of Georgia, Athens, GA 30602, USA. <sup>3</sup>Animal Health Trust, Lanwades Park, Newmarket, Suffolk CB8 7UU, UK. <sup>4</sup>School of Veterinary Medicine and Science, The University of Nottingham, Sutton Bonington, Leicestershire LE12 5RD, UK. <sup>5</sup>Department of Zoology, University of Cambridge CB2 3EJ, UK. <sup>6</sup>Cambridge Infectious Diseases Consortium, Department of Veterinary Medicine, Cambridge CB3 0ES, UK. <sup>7</sup>Fogarty International Center, National Institutes of Health, Bethesda, MD 20892, USA. <sup>8</sup>Department of Virology, Erasmus Medical Center, Rotterdam, Netherlands. <sup>9</sup>Center for Infectious Disease Dynamics, The Pennsylvania State University, University Park, PA 16802, USA. <sup>10</sup>Department of Ecology and Evolutionary Biology and Woodrow Wilson School, Princeton University, Princeton, NJ 08540, USA.

\*To whom correspondence should be addressed. Email: awpark@uga.edu

epitopes of the HA, the probabilities of becoming infected and infectious are close to 1. The infectious period shows a steady increase with degree of mismatch, increasing to around 5 days in unvaccinated control animals. All control (naïve) animals became infected and infectious. Reanalysis of a human influenza challenge study (12) reveals a qualitatively similar trend between  $p$  and  $a$  [see (11) for details].

Deterministic and stochastic models (11), parameterized from the equine data (Fig. 1), were used to explore the risk of outbreaks in vaccinated populations, as a function of immune escape. We consider the spread of infection in populations where all 1000 hosts are given the same imperfect vaccine and one infectious individual is introduced into the population;  $R$  begins to exceed 1.0 at  $a \geq 2$  (i.e., at least two amino acid differences). Coinciding with this, the deterministic model and the worst-case scenario from the stochastic model begin to show large outbreaks (Fig. 2A), which increase in size as  $a$  increases. For  $a < 2$ , we only see stuttering chains of transmission, with ~5% of the population infected in the worst-case scenario. The stochastic model shows that large outbreaks only become the more likely outcome (50th percentile for outbreak size) for  $a \geq 7$  (Fig. 2A).

Because the switch from small to large outbreaks being more likely is a qualitative phenomenon (13), we can readily use it to demonstrate how the target vaccine coverage to attain herd immunity (14) increases as  $a$  between the vaccine and circulating strains increases (Fig. 2B). Similarly, when all hosts are vaccinated, there is a trade-off between  $a$  and the minimum value of  $R_0$  required to overcome the herd immunity effect (fig. S3).

Although influenza A demonstrates a strong correlation between genetic changes in HA and resulting antigenic phenotype (3), punctuation in the antigenic evolution of human influenza viruses indicates that certain amino acid changes have a greater antigenic effect than others (3, 7). The trends observed in the epidemiological traits measured in the equine challenge studies were still evident when antigenic distances (table S4) rather than amino acid differences in antigenic sites were used as the explanatory variable (fig. S4).

Equine influenza strains from the Eurasian ( $n = 17$  strains) and American ( $n = 24$  strains) H3N8 lineages (table S5) were used to compare the use of genetic or antigenic distance to characterize epidemic probability (11). Distances were calculated from Newmarket/2/93, which was chosen as a reference strain because it represents the central point of the Eurasian antigenic cluster (Fig. 3A) and was used in several of the challenge studies. These data were used with the stochastic population model to consider the scenario in which a population of 1000 individuals is vaccinated with the reference strain and one individual (infectious with another strain) is introduced into the population. Sizing and coloring the infecting strain according to model predictions

of outbreak probability (Fig. 3B) clearly shows the differential risk depending on whether the vaccine and infecting strains are from the same antigenic cluster. When the vaccine and infecting strains come from within a cluster, large outbreaks are rare. Conversely, when the two strains are from different clusters, large outbreaks occur with a probability approaching 0.5 and can result in infection of around 70% of the population (fig. S6). This finding mirrors the observation that unexpectedly large outbreaks occur in vaccinated equine popula-

tions when infecting and vaccine strains are from different antigenic clusters (15). Sometimes a strain may be predicted to cause a large epidemic on the basis of genetic data despite a vaccine and infecting strain pair appearing to be antigenically similar (Fig. 3B, I) and vice versa (Fig. 3B, II). Overall, though, the model's risk predictions based on genetic distance between vaccine and challenge strains form low and high-risk groups, which are generally consistent with the strain groupings based on antigenic distance.

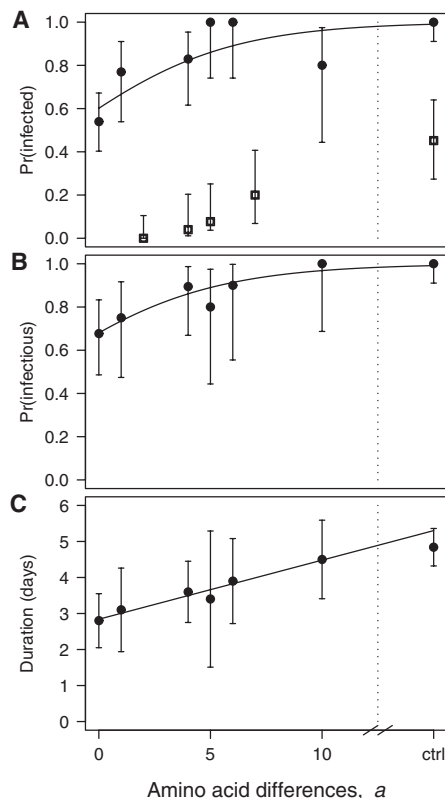


**Fig. 1.** Results from experimental infection of vaccinated hosts. Increasing the number of amino acid differences in HA epitopes between vaccine and challenge strains affects (A) the probability of becoming infected, (B) the probability of becoming infectious, and (C) the infectious period. Closed circles show the group means from the equine challenge studies and open squares the group means for probability of becoming infected in the human challenge study of Potter *et al.* (12). Error bars represent 95% confidence intervals. Solid lines are logistic [(A) and (B)] and linear (C) regressions, with parameters given in table S4. Control (unvaccinated) data are shown but were not used in the regression parameter estimation.

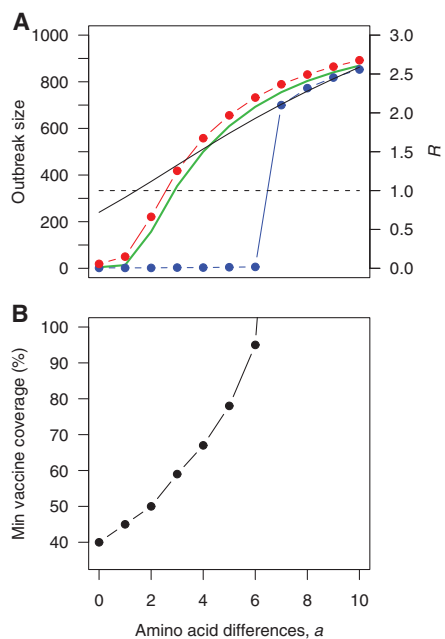


**Fig. 2.** Results from population models. (A) Outbreak size and effective reproductive number ( $R$ ) in a vaccinated population of 1000 individuals as a function of the number of amino acid differences in HA epitopes of the vaccine and circulating strains. The green line shows the deterministic model prediction for outbreak size, and the solid black line shows the value of  $R$ . Five thousand stochastic simulations were ranked by outbreak size. Red circles denote 95th percentiles and blue circles 50th percentiles (median). (B) Closed circles show the minimum vaccine coverage necessary to prevent large outbreaks from being the most likely outcome as a function of the number of amino acid differences between the vaccine and circulating strains (assuming  $R_0 = 3.0$ ). Details of model implementation are given in (11).

For seasonal influenza, previous exposure to virus as a result of vaccination and infection results in a heterogeneous profile of population immunity. We derive an expression for  $R$  when the host population is heterogeneous with respect to partial cross-immunity to a circulating strain ( $I$ ) which shows how  $R$  depends on the mean and variance of the number of amino acid differences between the infecting strain and the strains against which a given host's immune system is primed. In addition,  $R$  depends on the term  $\frac{\partial^2 R}{\partial a^2}$ , which captures the details of how the important components of cross-immunity change as a function of the number of amino acid differences. The degree of heterogeneity in the population, measured by  $\text{var}(a)$ , can play a crucial role in determining epidemic risk ( $I$ ) (fig. S6).

This research is also pertinent to the use of vaccines to control pandemic influenza. Baseline predictions of a pandemic with no intervention could be estimated using the model parameterized with data from experimental infection of immunologically naïve animals. Prepandemic vaccines have the advantage that they can be used prophylactically, and can be rapidly dispatched to at-risk populations in the event of a crisis, but are unlikely to be a perfect match to circulating strains ( $I$ 6). Our work shows that even these vaccines can provide a benefit to the population (providing  $a$  is not too large); increasing the proportion of the population vaccinated can offset an imperfect match between strains (Fig. 2B). In other models, a trade-off has been demonstrated between vaccine coverage and efficacy (foot-and-mouth disease) ( $I$ 7), or dose (pandemic influenza) ( $I$ 8). Also, models using vaccination in conjunction with antivirals to control pandemic influenza show that low-efficacy vaccines augment population-level protection ( $I$ 9).

This study illustrates the power of *in vivo* infections of natural hosts to illuminate the dynamics of incompletely immunizing pathogens. Specifically, it is the first to explicitly measure how heterogeneity between prevailing immunity and a viral

escape mutant influences transmission (through components of the effective reproductive number) and hence epidemic potential in a natural host. This calibration should reinforce modeling studies that relate genetic and antigenic change of influenza virus to ensuing large-scale patterns, including cluster transition rates, seasonal attack rates, and refractory periods ( $I$ 7).

Although the model uses data to estimate the dependence of key epidemiological parameters on the genetic distance between vaccine and infecting strains, certain assumptions were necessary ( $I$ 1). Because transmission was not explicitly measured in the experiments, we need to assume a baseline transmission rate; this corresponds to  $R_0 = 3.0$ , which is in line with upper-bound estimates for human influenza A ( $I$ 20,  $I$ 21) and is in the range of a recent estimate for EIV in stabled racehorses ( $I$ 22). Qualitative predictions of the model are robust to changes in this parameter (e.g., fig. S3). The infectious period may be overestimated because it is measured as duration of viral shedding, which ignores the possibility that titers of virus shed may be below an infectious dose, particularly in the early and late stages of this period ( $I$ 23). The model assumes that parameters  $p$ ,  $q$ , and  $d$  vary independently with  $a$ . The data suggest that this is generally true ( $I$ 1). There is some evidence of correlation between  $q$  and  $d$  (possibly mediated by some unmeasured immunological effect). Consequently, an alternative population model is tested embodying this covariance; it shows that results are unaffected by this modification ( $I$ 1). The antibody-binding epitopes of H3 HA were proposed for human influenza A ( $I$ 24). Although the antigenic sites of equine H3 HA have not been mapped completely, from the data available to date, it is believed that they are equivalent to those proposed for human H3 HA because the human and equine H3 influenza viruses share a common ancestry ( $I$ 25).

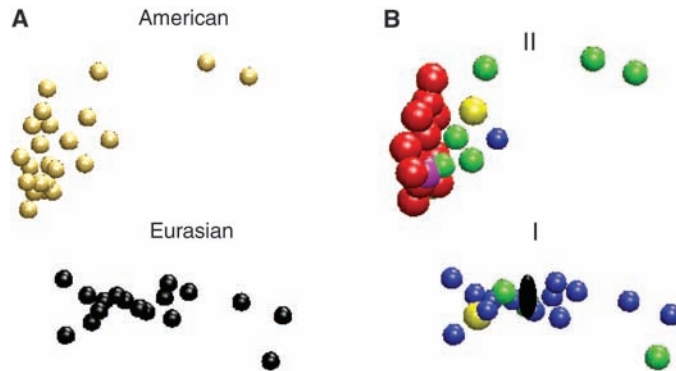
The synthesis of disease data at different scales (amino acids up to group-level infection studies) has illustrated how herd immunity and

immune escape are related in systems with antigenically complex pathogen and host structures. The ultimate goal is to directly link these results to epidemic dynamics, which is a realistic objective as influenza sequence data continues to accumulate. The ideas presented here could extend to a broad class of infections, including emerging, re-emerging and extant infectious diseases.

References and Notes

1. N. J. Cox, K. Subbarao, *Annu. Rev. Med.* **51**, 407 (2000).
2. D. Hobson, R. L. Curry, A. S. Beare, A. Ward-Gardner, *J. Hyg. (London)* **70**, 767 (1972).
3. D. J. Smith *et al.*, *Science* **305**, 371 (2004).
4. N. M. Ferguson, A. P. Galvani, R. M. Bush, *Nature* **422**, 428 (2003).
5. J. R. Gog, J. Swinton, *J. Math. Biol.* **44**, 169 (2002).
6. B. T. Grenfell *et al.*, *Science* **303**, 327 (2004).
7. K. Koelle, *Science* **314**, 1898 (2006).
8. R. M. Anderson, R. M. May, *Infectious Diseases of Humans: Dynamics and Control* (Oxford Univ. Press, New York, 1991).
9. M. J. Studdert, *Virus Infections of Invertebrates* (Elsevier, New York, 1996).
10. J. M. Daly *et al.*, *Vaccine* **22**, 4101 (2004).
11. Materials and methods are available as supporting material on Science Online.
12. C. W. Potter, R. Jennings, J. Nicholson, D. A. J. Tyrrell, K. G. Dickinson, *J. Hyg. (London)* **79**, 321 (1977).
13. I. Näsäll, *Epidemic Models: Their Structure and Relation to Data* (Cambridge Univ. Press, Cambridge, 1995).
14. P. E. M. Fine, *Epidemiol. Rev.* **15**, 265 (1993).
15. J. R. Newton, K. Verheyen, J. L. N. Wood, P. J. Yates, J. A. Mumford, *Vet. Rec.* **145**, 449 (1999).
16. N. M. Ferguson *et al.*, *Nature* **442**, 448 (2006).
17. M. J. Keeling, M. E. J. Woolhouse, R. M. May, G. Davies, B. T. Grenfell, *Nature* **421**, 136 (2003).
18. S. Riley, J. T. Wu, G. M. Leung, *PLoS Med.* **4**, e218 (2007).
19. I. M. Longini *et al.*, *Science* **309**, 1083 (2005).
20. C. Mills, J. Robins, M. Lipsitch, *Nature* **432**, 904 (2004).
21. J. Wallinga, M. Lipsitch, *Proc. R. Soc. London Ser. B. Biol. Sci.* **274**, 599 (2007).
22. K. Satou, H. Nishiura, *J. Eq. Vet. Sci.* **26**, 310 (2006).
23. D. C. Wiley, J. J. Skehel, *Annu. Rev. Biochem.* **56**, 365 (1987).
24. J. A. Mumford, D. Hannant, D. M. Jessett, *Equine Vet. J.* **22**, 93 (1990).
25. R. S. Daniels, J. J. Skehel, D. C. Wiley, *J. Gen. Virol.* **66**, 457 (1985).
26. We are grateful to R. Pyhälä, National Public Health Institute, Finland, for providing the HA1 sequence for A/Finland/74 (H3N2) and L. Yipu, National Institute for Medical Research, UK, for providing a sample of A/Scotland/74 (H3N2) from which we obtained the HA1 sequence. We also thank J. Gog, S. Gandon, J. Drake, P. Rohani, and Y. Michalakis for helpful discussions. Financial support came from Horserace Betting Levy Board (A.P. and J.D.), University of Georgia (A.P.), Cambridge Infectious Diseases Consortium (N.L.), NIH Director's pioneer award DP1-OD000490-01 (D.S.), European Union 223498 (D.S.), Human Frontiers Science Program (D.S.), Defra grant VT0105 (J.W.), Alborada Trust (J.W.), Research and Policy for Infectious Disease Dynamics program of the Science and Technology Directorate, Department of Homeland Security (J.W. and B.G.), NIH grant R01GM083983-02 (B.G.), NSF grant 0742373 (B.G.), Fogarty International Center, and NIH (B.G., D.S., J.W.). The authors declare no competing financial interests.

**Fig. 3.** A sample of equine influenza strains positioned in a three-dimensional antigenic space, where the antigenic phenotype is determined by antigenic cartography of haemagglutination inhibition assay titers (3). Strains are colored according to (A) phylogenetic grouping [black strains belong to the "Eurasian" lineage and gold strains to the "American" lineage ( $I$ 10)] and (B)



stochastic model predictions for the probability ( $s$ ) of a large outbreak (determined by a histogram analysis of 1000 replications of the model) in a population of 1000 individuals vaccinated with the strain shown as a black ellipsoid in cluster I, into which one individual (infectious with one of the strains shown in the figure) is introduced. Increasing sphere size represents increasing probability of a large outbreak. This is also color coded where probabilities are blue,  $s = 0.0$ ; green,  $0.1 < s < 0.2$ ; yellow,  $0.2 < s < 0.3$ ; red,  $0.3 < s < 0.4$ ; magenta,  $0.4 < s < 0.5$ .

Supporting Online Material

www.sciencemag.org/cgi/content/full/326/5953/726/DC1  
 Materials and Methods  
 Figs. S1 to S7  
 Tables S1 to S5  
 References

7 May 2009; accepted 15 September 2009  
 10.1126/science.1175980